

Original Article

Healing of cancellous fracture in a novel mouse model

Duanyang Han*, Na Han*, Yixun Chen, Peixun Zhang, Baoguo Jiang

*Department of Orthopedics and Trauma, Peking University People's Hospital, China. *Equal contributors and co-first authors.*

Received July 15, 2015; Accepted October 12, 2015; Epub November 15, 2015; Published November 30, 2015

Abstract: Fractures are one of the most prevalent clinical conditions worldwide. Among them, cancellous fracture is a major cause of extremities fractures. Unfortunately, it is largely unknown about how is the healing of cancellous fracture. In the current study, we present a novel cancellous fracture mice model, which successfully mimic clinical cancellous fracture scenario. Next, we showed that the newly repaired trabeculae in fracture healing zone were thicker than normal bone tissue with more sufficient local blood supply. There are more osteoclasts reside in the fracture healing zone than normal bone tissue and these osteoclasts distributed more closely and densely. Moreover, the early repairing bone mass in fracture healing zone was not fully collagen loaded as normal bone tissue. Comparing to similar cell proliferation activity, upregulated local cell function play more important role in the cancellous fracture repair.

keywords: Cancellous fracture, mouse model, fracture healing

Introduction

Skeletal fractures are the most frequently reported medical conditions in developed country such as the United States and the second-greatest cause of disability worldwide [1]. Fracture healing is accomplished by closing the fracture gap with bone tissue, which recapitulates many aspects of embryological skeletal development [2]. Among various types of fractures, cancellous fracture is a major cause of extremities fractures [3-6]. Clinically, cancellous fractures heal in a much more rapid fashion and have several unique features comparing with cortical fractures. This difference may due to the unique microarchitecture and ultrastructure of cancellous bone over cortical bone. In cortical bone, typical osteon structures are surrounded by cement lines and interstitial tissue [7, 8]. However, in cancellous bone, interstitial tissue is present in the central regions of trabeculae, distant from the trabecular surfaces [8]. Moreover, the orientation of cement lines in cancellous bone differs from that in cortical bone since cancellous bone does not exhibit osteons structures [9]. Furthermore, remodeling in cancellous bone causes the generation of resorption cavities, which unique from the callus forming process of cortical fracture healing [10, 11]. Although numerous stud-

ies using various animal models have been performed to study fracture healing, most authors only address the cortical fracture healing mechanisms [12]. Healing mechanisms of cancellous fractures are still poorly understood. Moreover, no animal model, which can successfully mimic clinical scenario, is currently available to facilitate specialized cancellous fracture healing studies. In this study, we first designed a specialized cancellous animal model on mice. Furthermore, using this novel model, we demonstrate that, in cancellous fracture healing, the activity of local cells including secreting fibronectin material and osteoclast activity play more important roles than the amount of local cells.

Materials and methods

Establishment of mouse cancellous fracture model

Total of 30 Male Balb/c mice (8-10 weeks old) weighing approximately 26 g were obtained from vital river laboratory (location?). All of the animal experimental procedures were performed under the Institutional Animal Care Guidelines and approved ethically by the Administration Committee of Experimental Animals, Peking University People's Hospital, where the ani-

A mouse model to study cancellous fracture healing

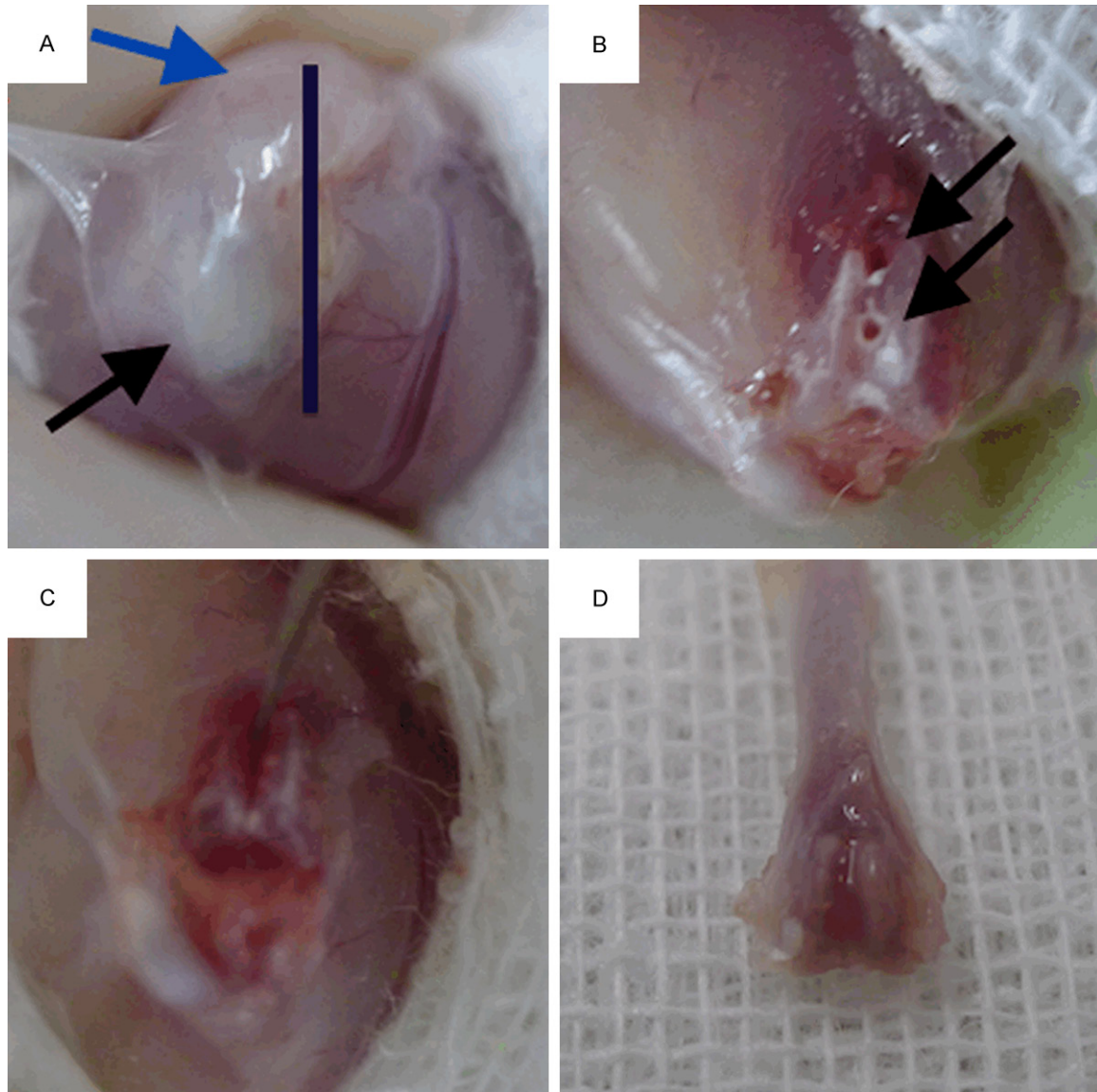


Figure 1. (A) Mouse cancellous fracture model surgery. The bar indicates the incision site. Incision should fully expose the ligamentum patellae and musculi quadriceps femoris anatomical structures. (Shown by black and blue arrows respectively); (B) Two parallel leading holes, as indicated by two black arrows, were made at the intercondylar fossa to lead the direction of artificial fracture line; (C) After fully connected both leading holes with the scalpel tip, gently twist the scalpel in a “key open lock” maneuver to make a single stable fracture line; (D) The distal half of femur was collected and submitted to subsequent stains. Gross anatomy showed that the cancellous fracture line had mostly healed by day 7.

mals were raised and studied. Left leg of every mouse was made into the fracture model side and right leg was taken as the normal control side. The surgical procedures were performed as following. The anesthesia was carried out by an intraperitoneal injection of 10% ketamine and 2% xylazine. As shown in **Figure 1A**, an parallel incision was made medially to the left ligamentum patellae, the incision should involve at least 4 mm of the lower musculi quadriceps femoris in order to fully exposure the surgical

field for next steps. Next, bluntly separate the patellae together with the intact ligament from the underneath tissue and push them laterally with gentle to fully expose the distal femoral head. We used U-100 insulin syringe needle as a mini-drill and made two leading holes at the intercondylar fossa, which drilled parallel into the femoral medullary cavity (Shown in **Figure 1B**). Make sure both leading hole were created along the same direction and on the same sagittal plane. After both leading holes

A mouse model to study cancellous fracture healing

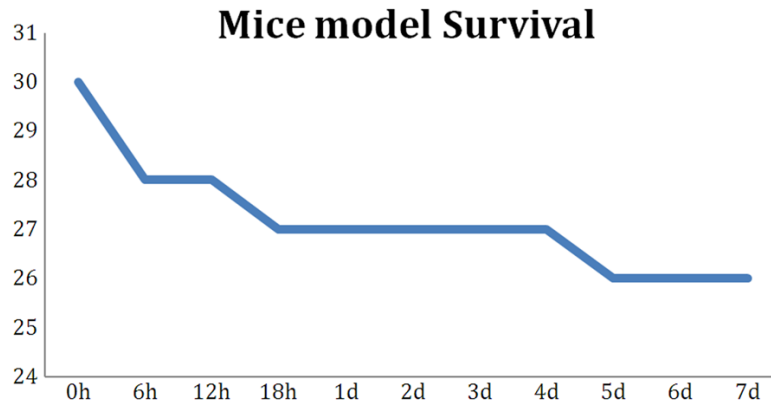


Figure 2. Our novel mouse cancellous fracture model shows excellent survival rate. In total of 30 mice, only 4 deaths incidence occurred. Three deaths happened in the first 24 h after surgery. One mouse was euthanized due to wound infection (bite open) on day 5.

were properly made, we gently pushed the tip of a sharp scalpel (size #26) into the first leading hole with blade toward the second leading hole as shown in **Figure 1C**. When the blade had fully arrived the second leading hole, gently twist the scalpel like a “key open lock” maneuver. Because of the exit of two parallel leading holes, a single straight fracture line was made along the direction of leading holes. Examined both medial and lateral condyle bones to exclude the existence of unstable displaced fracture before wound closure. A properly made fracture model has a single stable intercondylar fracture line. All procedures should be finished under sterile condition. Several practices are necessary to fully master all procedures.

Histology analysis

At day 7 after model surgery, all Mice were euthanized and fractured or control femors were removed and dissected free from surrounding musculature using a dissecting microscope. Bones collected for hematoxylin/eosin (H&E) staining and immunohistochemistry were fixed in either 70% ethanol for 48 h or in 10% neutral buffered formalin (Fisher Scientific) for 24 h and stored at 4°C in 70% ethanol. Bones were decalcified in 10% EDTA at 4°C for 3-7 days (determined by physical testing) before paraffin embedding, sectioning, and H&E staining using standard protocols.

Masson's trichrome staining

Sections (4 µm thick) were stained according to the masson kit protocol. Briefly, the sections

were dewaxed, dehydrated in graded alcohols and stained by hematoxylin for 3 min. After washing with running water, sections were differentiated in a 1% hydrochloric acid alcohol solution. Sections were then stained in warm Ponceau acid fuchsin solution for 3 min, washed with distilled water, and differentiated in a 1% phosphomolybdic acid solution for 1 min. After wiping the phosphomolybdic acid residue from the slides, the sections were stained in 2% aniline blue solution for 1 min.

Sections were dehydrated in graded alcohols, dried with cold air, and mounted in neutral resin.

Trap staining

To preserve Trap activity, all procedures were conducted at 4°C. The bones were switched from xylene to methyl methacrylate (MMA; Fluka/Sigma-Aldrich) and maintained at -20°C for 24 h. This step was followed by two 24 h baths of 5 ml MMA with 80 µl polymerization activator (5% vol/vol N, N-dimethylaniline in isopropyl alcohol; Sigma-Aldrich). The bones were then embedded in 24 ml of MMA with 240 µl polymerization activator overnight in a water bath at 4°C. After each change of MMA, the samples were maintained in a vacuum to facilitate penetration for 1 h before storage at -20°C. Osteoclasts were identified by immunostaining of Trap on 10-µm-thick sections. Trap activity was revealed by incubating the sections in a solution of naphthol-1-phosphate sodium salt and fast violet (Sigma-Aldrich) in acetate buffer (pH 5) overnight at 4°C. The enzymatic reaction was stopped by immersing the sections in sodium fluoride for 30 min, and the bone matrix was counterstained with aniline blue (Sigma-Aldrich). The osteoclasts were identified as red-colored cells in direct contact with the bone matrix. Pictures of all sections were captured on a microscope (Carl Zeiss MicroImaging).

Immunohistochemistry

Ki-67 and fibronectin were detected on formalin-fixed, paraffin-embedded sections by using

A mouse model to study cancellous fracture healing

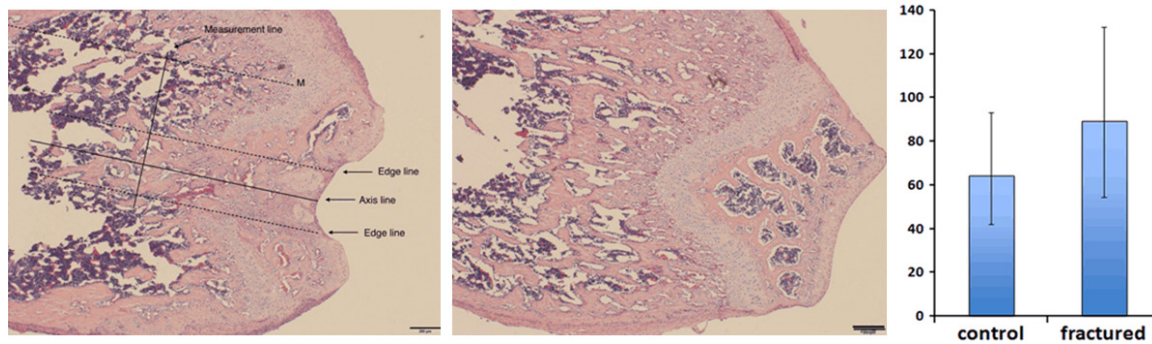


Figure 3. Fracture line was well maintained parallel to the axis of the femur shaft. Fracture healing zone was defined on the left figure. Measurement line was also defined and indicated. Trabecular width was measured using Image-Pro Plus software. Newly repaired trabeculae were significantly thick than normal bone tissue ($P < 0.05$).

primary antibodies both from Abcam, Cambridge. Briefly, slides were baked at 55°C for overnight, deparaffinized in two washes of xylene, and rehydrated in a decreasing ethanol gradient. Antigen retrieval was performed using 0.5% trypsin for 30 min at 37°C in a humidified chamber. Endogenous peroxidases were deactivated with 3% H_2O_2 for 30 min, and sections were blocked in PBS supplemented with 0.1% Triton-X (Sigma-Aldrich), 2% goat serum (Gibco BRL), and 1% BSA (Sigma-Aldrich) for 20 min at room temperature. Sections were incubated with primary antibody (1:100 dilution for Ki-67; 1:100 dilution for fibronectin) in Antibody dilution water overnight at 4°C. The following morning, the sections were washed in PBS and incubated with anti-rabbit IgG-HRP secondary antibody (GTVision) in PBS (1:1000 dilution) for 45 min at room temperature. After washing with PBS, HRP activity was detected using a DAB substrate kit (SK-4100; Vector Laboratories) according to the manufacturer's instructions.

Statistical analysis

All measurement of trabecular width, blood supply transection area is finished using Image-Pro Plus software. Unless specifically illustrated, all measurement data were collected from 15 pairs of samples, 4 trap staining slides for each pair and 2 random microscopic fields (20x). The SPSS 17.0 software package (SPSS Inc., USA) was used for statistical analysis. Experimental data were compared using the Student's t test and One-Way ANOVA followed by Student-Neuman-Keuls test. Differences were considered statistically significant when $P < 0.05$.

Results

Our novel cancellous fracture model exhibit stable and repeatable histologic morphology

We first evaluate our novel cancellous fracture (what are the evidence to confirm it is indeed a cancellous fracture?) model by assessment the overall condition of the mice. The overall survival rate by 7 day is 86.7% that shows our animal model is a substantially safe and dependable procedure to use (**Figure 2**). Especially considering most of the fatality incidents were caused by general anesthesia and happened in the post-anesthesia phase, our animal model surgical procedure itself is even safer than the overall survival rate shows. Generally, all mice recover to normal activity and appetite from the second day after surgery. Only one (3.3%) of the mice developed wound infection, which were caused by biting the suture open in early days after surgery. On the 7 day after surgery, all mice were sacrificed and both femurs were collected for further evaluations. From gross anatomy, we can observe that the fracture line was mostly repaired and anatomical shape of the fractured femur was well preserved (**Figure 1D**). This finding joint with the early recovery of normal activity to prove that our specialized cancellous fracture model create stable fracture line which remit the necessity of extra external or internal fixation.

To be specific, we defined the fracture healing zone that we focused on in the following series of studies. As shown in **Figure 3**, first made an axis line along the sagittal plane, passing the middle point of both condyles. Then, we made two parallel dashed edge lines each of which

A mouse model to study cancellous fracture healing

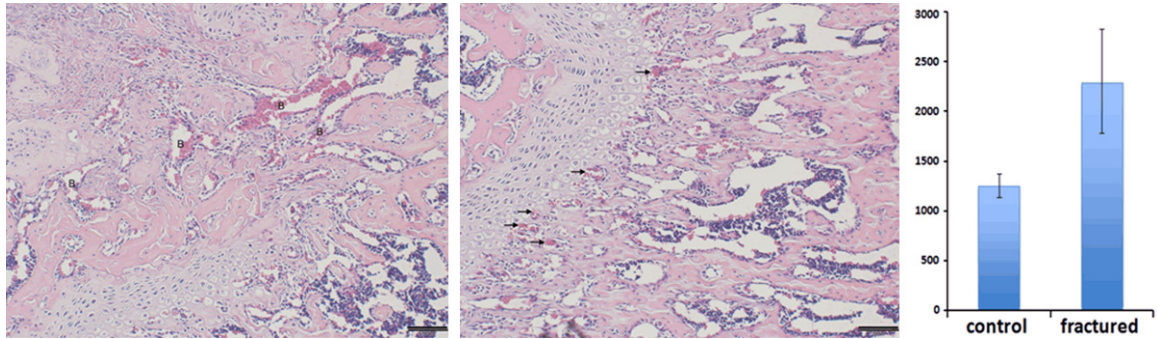


Figure 4. More sufficient blood supply was found in the fracture healing zone and distribution of local blood supply were altered. (Left) large blood sinus was shown in the fracture region (Shown by letter B); (Middle) much smaller blood vessels were found in the normal bone tissue and majority of the blood supply lied along the proximal edge of the epiphysis plate (Shown by small arrows); (Right) Blood supply transection area of fracture healing zone was significantly larger than normal bone tissue ($P < 0.05$).

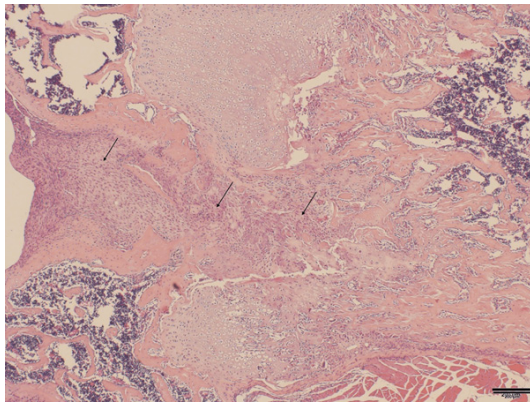


Figure 5. Large number of mononuclear cells was found in the fracture healing gap (Arrow).

located 200 µm to the axis line. We refer the zone between both edge lines as “fracture healing zone”. Additionally, we made another dashed assistance line, parallel to axis line, from the highest point of the epiphysis. Next, made a measurement line vertically passing the assistance line. The distance between the highest spot of the epiphysis and the measurement line was 800 µm. All trabeculae intersecting the measurement line in the fracture healing zone would be the candidates for subsequent trabecular width measurement.

The histologic evaluation confirmed the success of our specialized cancellous fracture model. A clean and stable single fracture line was seen on almost every specimen. Fracture line direction was precisely maintained parallel to the axis of the femur shaft (**Figure 3**). At day 7, the fracture wound had been mostly repaired with woven bone with typical cancellous-like architecture. However, distinguished from the

classical intramembranous or endochondral ossification process, the cancellous fractures heal in a unique pattern. By day 7, the average trabeculae width of fractured zone is 89.5 µm. Comparing to the normal trabeculae width (64.2 µm), the trabecular width of cancellous fracture zone is 39.4% thicker its normal counterpart ($P < 0.05$). This finding indicate that the recovery of cancellous bone micro-architecture may first require “over-ossification” in the bone marrow cavity to form a healing ossification mass. Then, secondary bone catabolism process, featured by osteoclast activity, was turned on to resorb the redundant bone mass. We hypothesize that cancellous fractures heal in a unique “carving mechanism”. How this carving process is regulated during the fracture healing process to restore unique cancellous micro-architecture is still poorly understood. As we previously reported, our team observed similar cancellous healing pattern on rabbit model [13]. The trabecular width data of current mice model subject to the same trend with our previous rabbit model. Moreover, comparing to normal cancellous trabecular bone, more abundant local blood supply could be seen in newly repaired cancellous trabecular zone (**Figure 4**). The average blood vessel transection area is 2288 µm² per microscopic field (10x) in the fracture healing zone, which is 82.8% higher comparing to the normal bone tissue (1252 µm²) ($P < 0.05$). Furthermore, inflammatory cells were found in the fracture wound at day 7, which suggest the inflammatory reaction may play a role in the regulation and coordination of cancellous bone healing process, such as dead bone removal and new bone synthesis (**Figure 5**).

A mouse model to study cancellous fracture healing

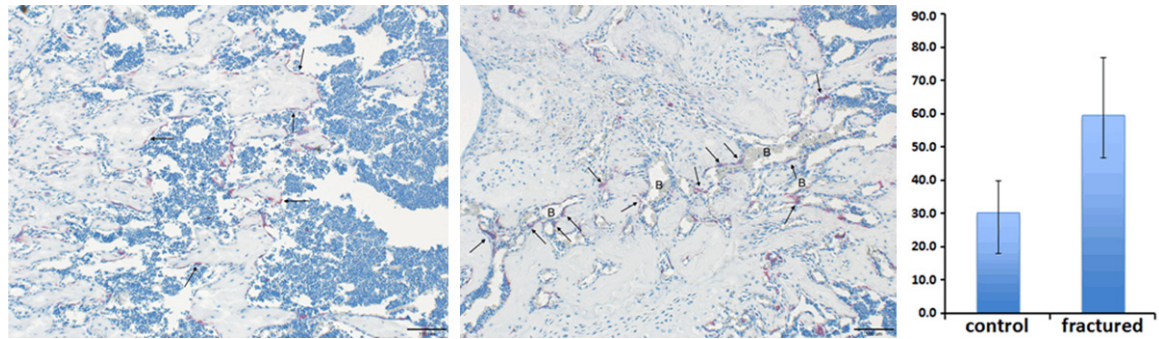


Figure 6. (Left) More osteoclasts (red stained spot) localized in the fractured zone and gathered more densely around the local blood supply (Arrows); (Middle) fewer osteoclasts were found in the normal bone tissue and scattered evenly along trabecular surfaces (Arrows); (Right) osteoclast number in fracture healing zone was significantly higher than normal bone tissue ($P < 0.05$).

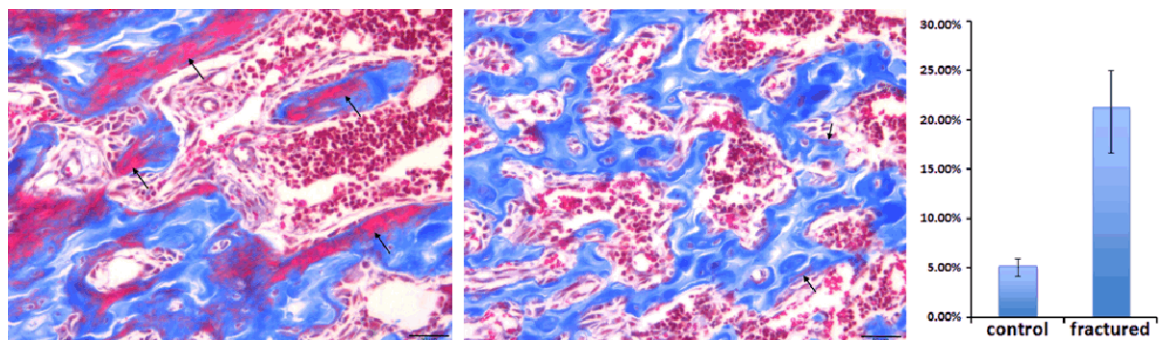


Figure 7. Newly repaired trabeculae are not fully collagen loaded (blue stain represent collagen). (Left) larger amount of new trabeculae were less collagen loaded in the fracture healing zone by day 7 (Arrow); (Middle) only very tiny part of the normal trabeculae were not fully collagen loaded which was a sign of normal bone remodeling process (Arrow); (Right) immature trabecular area percentage of fracture region were significantly higher than normal bone tissue ($P < 0.05$).

More osteoclasts reside in fracture zone support the carving mechanism theory

To evaluate our carving repair hypothesis, we next used trap staining to address osteoclast activity in the newly repaired cancellous trabeculae. Trap staining revealed that osteoclast is more densely distributed in the newly repaired trabecular bone tissue than normal trabeculae (**Figure 6**). To quantitatively account for the differences between newly repaired and normal tissue, we performed osteoclast counting in fracture healing zone from each slide. Statistical analysis revealed that the average osteoclast number in newly formed trabecular region was almost 2 fold higher than that in normal tissue ($P < 0.05$). Interestingly, we also observed that, in the fracture zone, osteoclasts were more tend to distribute on the interface between bone tissue and blood sinuses or blood vessels (**Figure 6**). In contrast, osteoclasts were more evenly distributed on the surfaces of trabecu-

lae and no significant correlation could be found between osteoclast distribution and local blood supply (**Figure 6**). In consistent with our carving repair hypothesis, these findings demonstrated that, comparing to normal trabecular bone, the osteoclast number and viability is upregulated in the newly formed trabecular bone tissue on day 7, which suggest that the resorption of the over-ossified repairing bone mass from the early healing period, in another word “carving”, is one major feature of the intermediate healing period.

Substantial amount of early-synthesized bone tissue in cancellous fracture zone is immature

We next performed Masson’s trichrome staining aiming to assess local chondrocyte participation in the cancellous fracture healing and to detect the collagen accumulation in the newly repaired trabecular bone at day 7. Our staining data demonstrated that large number of imma-

A mouse model to study cancellous fracture healing

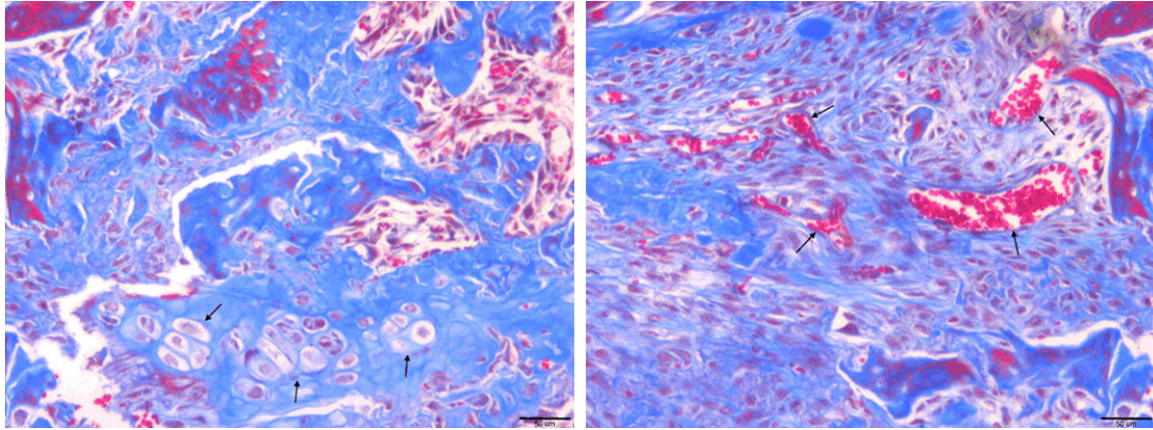


Figure 8. (Left) chondrocyte-like cell colonies were found in the fractured region (Arrow); (Right) sufficient local blood supply in the fracture healing zone (Arrow).

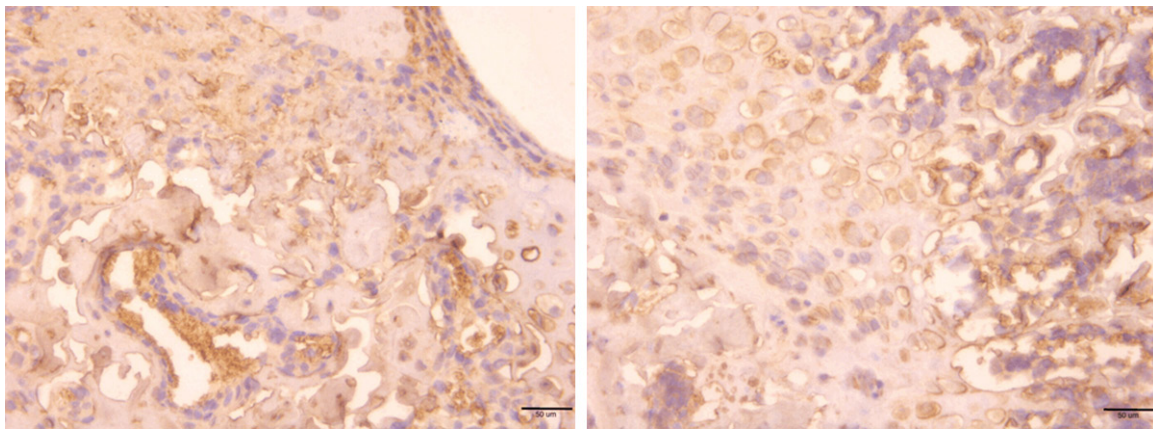


Figure 9. Ki-67 positive cells were seldom observed in both fractured (Left) and normal (Right) bone tissue, which suggested the cell proliferation activity was not upregulated in the fracture healing zone by day 7.

ture trabecular bone tissue exists in the fracture wound area, which characterized newly repaired trabecular bone tissue from normal control group (**Figure 7**). In the normal trabecular bone tissue, collagen material is evenly deposited on majority of the trabecular structures with few exceptions (**Figure 7**). In contrast, in the fracture healing zone, many newly formed trabecular structures are not fully collagen loaded. Additionally, large amount of blood sinus and vessels were found adjacent to the poor collagen loaded regions (**Figure 8** right). This finding emphasized a positive relationship between cancellous bone reshaping and blood supply restoration. To quantify our observation, we performed statistical analysis on our masson staining slid. The insufficient collagen loaded trabecular area percentage is 21.3% in the fracture healing zone, which is

16.1% higher than data from normal bone (5.2%) ($P < 0.05$). Furthermore, we also found a few chondrocyte-like cell colonies in the fracture healing zone (**Figure 8** left), which suggest that endochondral ossification have potential to participate in cancellous fracture healing and restoration of the local micro-architecture.

Upregulated local cell function play more important role than cell proliferation

As our histomorphologic analysis revealed, there were large amount of mononuclear cells exist in the cancellous fracture healing zone whose nature and cellular function are still poorly understood. Next, we used immunohistochemistry staining targeting on Ki-67 and Fibronectin protein respectively. Ki-67 is a nuclear antigen that is used to detect proliferating cells. Five random fields (20 \times) in 15 pairs of

A mouse model to study cancellous fracture healing

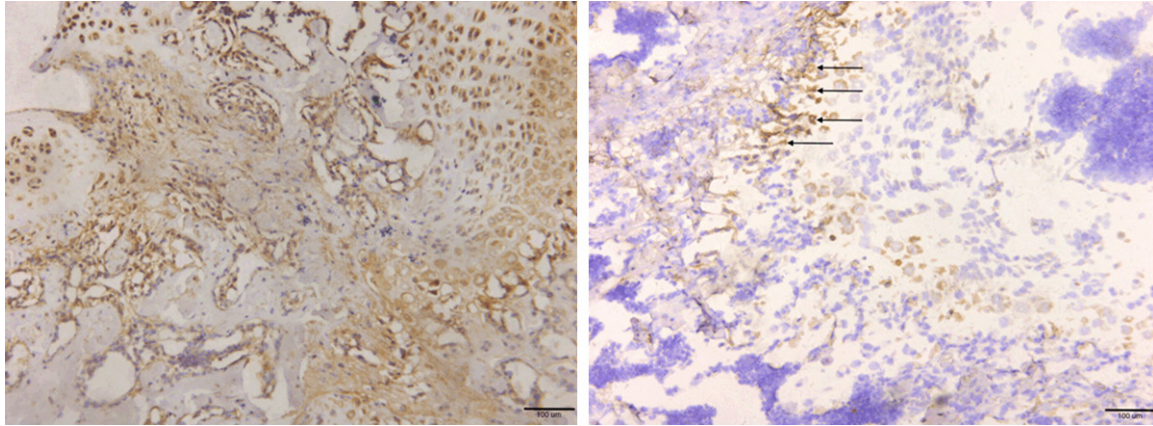


Figure 10. (Left) significantly upregulated fibronectin expression in the matrix of the fracture healing zone. In contrast, (Right) fibronectin expression in normal bone tissue was low and mostly localized along the proximal epiphyseal edge (Arrow).

samples were selected from fracture healing zone or the normal trabecular zone respectively, and Ki-67-positive cells were counted (**Figure 9**). Ki-67-positive cells were seldom observed in both cancellous fracture (1.5 ± 0.02) and normal bone tissue (1.3 ± 0.4) sections ($P > 0.05$). This finding demonstrates that local cell proliferation in the fracture healing zone is not significantly altered comparing to normal trabecular bone, which suggests that the cancellous fracture repair is not likely to be fulfilled by local cell, such as mesenchymal stem cell, proliferation at day 7. Furthermore, we next compared local fibronectin expression between fracture healing region and normal bone tissue. Fibronectin is secreted into the extracellular matrix by local functional cells. In the normal bone tissue, only sub-epiphyseal area showed regular moderate-level fibronectin stain in the extracellular matrix, which was a result of normal epiphyseal development and long bone elongation (**Figure 10** right). Majority of the matrix in the normal trabecular zone showed only very light fibronectin stain, which interpreted that fibronectin secretion is largely tuned down in the normal cancellous trabecular bone region (**Figure 10** right). On the contrary, local fibronectin accumulation is significantly upregulated in the extracellular matrix of newly repaired zone at day 7 (**Figure 10** left). Our data argue that, comparing to undifferentiated local cell proliferation activity among fracture healing zone and normal trabecular bone tissue, upregulated local cellular function, such as fibronectin secretion, play a more important role in cancellous fracture repair.

Discussion

Although cancellous fracture is a major type of extremities fractures in clinical practice [14-17], the specific healing mechanism of the cancellous fracture remain poorly elucidated. Majority of the scholars tend to ignore the histological differences between cancellous and cortical bone tissue and assume that cancellous fractures are repaired in the same mechanism as cortical ones. So far, most of the fractures healing studies focus on addressing healing mechanism of the long bone cortical fracture, however, the healing mechanism of cancellous fractures have not been thoroughly investigated. There even lacking a ideal animal model which mimicking real clinical scenarios and facilitate downstream researches to transgenic animal level. There are a few studies using relatively large animal, such as rabbits [13]. Nonetheless, they all require internal or external fixation, which make the large animal model hard and expensive to achieve. Moreover, the fracture line in these large animal model are made by high-energy bone sawing which inevitably produce over-heat to local neighboring wound tissue that may potentially interfere with the subsequent healing process. Additionally, it's very tough and expensive to make stable transgenic animal model using large animals. This disadvantage limits the downstream mechanism study on cancellous bone fractures. Currently for small animal model, the most widely use animal model is cancellous drilling model [18, 19]. Although this is a relatively easy model to make, a constant gap between two

A mouse model to study cancellous fracture healing

fracture parts during the whole healing processes cannot successfully mimic the real clinical fracture case. Also, many clinical metaphyseal cancellous fracture lines interrupt major joint cartilage surface, such as Muller's C1 type fractures of distal femur, which potentially facilitating joint cartilaginous cells to participate into subsequent healing mechanism. To reveal the unique healing mechanism of cancellous bone fractures, we designed a novel mice model, which can successfully mimic features of clinical cancellous fracture cases. Furthermore, comparing to other cancellous fracture models, our model produces a stable fracture that does not require any internal or external fixations. Also, the surgical procedures are highly repeatable and easy to learn. Excellent survival rate (86.7% at day 7) and quick recovery to normal activity also support this model to be an ideal animal model for specific cancellous fracture researches.

Facilitated by our novel animal model, we next performed histologic HE stain and osteoclast specific trap stain to study the cancellous fracture healing. At day 7, the newly repaired trabeculae in the fracture zone are averagely thicker than that of the normal cancellous bone tissue. A regular "building up" mechanism cannot explain the contradiction that why the new trabeculae are thicker than their normal counterpart at day 7. Inspired by this finding we hypothesized that the healing of cancellous fracture and restoration of the delicate micro-architecture of trabecular bone may have been through an "over-ossification" in the local bone marrow cavity around the fracture site which forming an ossification mass in the early phase of fracture healing. This early over-ossification bone mass acts like an internal fixation which stabilizes the local fracture wound and initiates the subsequent downstream repairing events. Next, after a tough early over-ossification bone mass is formed, bone mass catabolism mainly conducted by osteoclast bone absorption function starts to remove the redundant bone material which we referred as a "carving mechanism". Interestingly, our team has reported similar finding healing pattern on a rabbit model [13, 20]. In this study, our statistical analysis revealed that the newly formed trabecular region possessed about two fold more osteoclast number than that in normal tissue. Interestingly, we observed unique correlation between osteoclasts distribution and blood supply microvasculature in cancellous fracture healing

zone. Osteoclast distribution pattern is also altered in the fracture healing zone, which tends to associate more closely with blood supply resources. Since osteoclast is well recognized originate from circulating macrophage lineage [21, 22], our result strongly indicates that the trabecular carving mechanism may be initiated by subsequent osteoclast migrating into the early bone mass along with blood supply restoration process. The newly arrived osteoclasts from systemic circulation reinforce the local osteoclast-and-osteoblast balance towards the direction favoring the reestablishment of the unique cancellous micro-architecture of the fractured region.

To reveal the nature of newly repaired trabecular bone tissue, we employed Masson's trichrome staining to study collagen accumulation in bone tissue. We demonstrated a clear differentiated pattern of collagen deposition between normal and fractured cancellous bone tissue. Normal trabecular bone is mostly fully collagen loaded. In contrast, at day 7, poorly collagen loaded trabecular bone were still seen in the fracture region. This finding suggests that the early bone mass is produced despite without proper collagen accumulation and this feature may interact with subsequent bone carving mechanism which needs more detailed study to clarify. Another advantage of our current animal model is that it can evaluate the potential chondrocyte participation from joint capsule in the cancellous fracture repair. In deed, we found chondrocyte-like cell colonies exist in the fracture healing zone. However, more detailed investigation is needed to identify the exact role of this chondrocyte-like cell in the cancellous fracture healing.

From our HE staining data, we observed large amount of mononuclear cells exist in the cancellous fracture healing zone. Here in this study, we ask how these mononuclear cells gathered into the local fracture wound? Are they locally proliferating and behaved as certain sort of stem cell? Or, are they conducting their duty by upregulated local secretion? To answer these questions, we employed Ki-67 and fibronectin immunohistochemistry staining representing cell proliferative activity and cell secreting function respectively. Our data support that, comparing to normal bone tissue, cell proliferating activity was not significantly turned on in the fracture healing zone at day 7. In another word, cancellous fracture repair is not mainly depend-

A mouse model to study cancellous fracture healing

ing on local cell proliferation to boost the healing capacity at day 7. On the other hand, local fibronectin production is significantly upregulated in the matrix of fracture healing region. Despite majority of the previous studies focus on mesenchymal stem cell participation in the fracture wound healing, our data support the viewpoint that upregulated local cellular function play more important role in the healing mechanism of cancellous fracture.

Recently, inflammatory signaling, namely NF- κ B signaling, has been reported to exert an anti-anabolic effect on bone formation in differentiated osteoblasts. Moreover, inhibition of NF- κ B signal in differentiated osteoblasts significantly enhanced bone matrix formation and mineral density during postnatal bone growth [23, 24]. These evidences suggest that the inflammatory signaling pathways, such as NF- κ B signaling, may also play a vital regulating role in the fracture healing mechanism. Of interest, from our current study, we indeed observed large number of inflammatory cells gathered in the fracture-healing zone whose exact function was still unclear. Thus, in our further research, we will take advantage of our novel mice model and using specific gene knockout mice to reveal the detail relationship between local inflammatory signaling and cancellous fracture repair.

In summary, we first present a novel specific cancellous fracture model in the current study and prove that this is an easy, safe and repeatable model which can better mimic clinical cancellous fracture scenario like Muller's C1 type fracture. Using this specific cancellous fracture model, we showed that, controversial to normal concept, the newly repaired trabeculae in fracture zone were thicker than their normal counterpart with more sufficient local blood supply. Inspired by this finding, we hypothesize a novel "carving mechanism" for cancellous fracture healing. In support of this hypotheses, our trap stain data found that there are indeed more osteoclast reside in the fracture healing zone than normal bone tissue and these osteoclast distributed more closely and densely around local blood supply which argued that these osteoclasts were newly arrived to the fracture wound via local blood supply. Moreover, our masson stain confirmed that the early local bone mass is not fully collagen loaded as normal bone tissue, which was also potentially linked with subsequent carving mechanism.

Furthermore, we used both Ki-67 and fibronectin staining to assess the change of local cell proliferation and cell function. Our data showed that local cell proliferation in fracture healing zone was actually not altered. However, the fibronectin secreting function of local cells were indeed upregulated in the fracture zone. These finding suggest that local cell function stimulation rather than cell number swelling seems to play a more important role in the cancellous fracture repair. Future studies to address the detail regulatory signaling pathway will require the development of mouse line in which specific bone signaling pathway can be individually regulated.

Acknowledgements

This work was funded by Chinese National Ministry of Science and Technology 973 Project Planning (No. 2014CB542200 and 2014-CB542206); 863 project (No. SS2015AA020-501). The ministry of education innovation team (IRT1201); the National Natural Science Fund (No. 31271284, 31171150, 81171146, 30971526, 31100860, 31040043), and the Educational Ministry New Century Excellent Talents Support Project (No. BMU20110270).

Disclosure of conflict of interest

No.

Address correspondence to: Peixun Zhang and Baoguo Jiang, Department of Orthopedics and Trauma, Peking University People's Hospital, China. E-mail: zhangpeixun@bjmu.edu.cn (PXZ); jiangbaoguo@vip.sina.com (BJG)

References

- [1] Vos T, Flaxman AD, Naghavi M, Lozano R, Michaud C, Ezzati M, Shibuya K, Salomon JA, Abdalla S, Aboyans V, Abraham J, Ackerman I, Aggarwal R, Ahn SY, Ali MK, Alvarado M, Anderson HR, Anderson LM, Andrews KG, Atkinson C, Baddour LM, Bahalim AN, Barker-Collo S, Barrero LH, Bartels DH, Basáñez MG, Baxter A, Bell ML, Benjamin EJ, Bennett D, Bernabé E, Bhalla K, Bhandari B, Bikbov B, Bin Abdulhak A, Birbeck G, Black JA, Blencowe H, Blore JD, Blyth F, Bolliger I, Bonaventure A, Boufous S, Bourne R, Boussinesq M, Braithwaite T, Brayne C, Bridgett L, Brooker S, Brooks P, Brugha TS, Bryan-Hancock C, Bucello C, Buchbinder R, Buckle G, Budke CM, Burch M, Burney P, Burstein R, Calabria B, Campbell B, Canter CE, Cara-

A mouse model to study cancellous fracture healing

- bin H, Carapetis J, Carmona L, Cella C, Charlson F, Chen H, Cheng AT, Chou D, Chugh SS, Coffeng LE, Colan SD, Colquhoun S, Colson KE, Condon J, Connor MD, Cooper LT, Corriere M, Cortinovis M, de Vacarro KC, Couser W, Cowie BC, Criqui MH, Cross M, Dabhadkar KC, Dahiya M, Dahodwala N, Damsere-Derry J, Danaei G, Davis A, De Leo D, Degenhardt L, Dellavalle R, Delossantos A, Denenberg J, Derrett S, Des Jarlais DC, Dharmaratne SD, Dherani M, Diaz-Torne C, Dolk H, Dorsey ER, Driscoll T, Duber H, Ebel B, Edmond K, Elbaz A, Ali SE, Erskine H, Erwin PJ, Espindola P, Ewoigbokhan SE, Farzadfar F, Feigin V, Felson DT, Ferrari A, Ferri CP, Fèvre EM, Finucane MM, Flaxman S, Flood L, Foreman K, Forouzanfar MH, Fowkes FG, Franklin R, Fransen M, Freeman MK, Gabbe BJ, Gabriel SE, Gakidou E, Ganatra HA, Garcia B, Gaspari F, Gillum RF, Gmel G, Gosselin R, Grainger J, Groeger J, Guillemin F, Gunnell D, Gupta R, Haagsma J, Hagan H, Halasa YA, Hall W, Haring D, Haro JM, Harrison JE, Havmoeller R, Hay RJ, Higashi H, Hill C, Hoen B, Hoffman H, Hotez PJ, Hoy D, Huang JJ, Ibeanusi SE, Jacobsen KH, James SL, Jarvis D, Jasrasaria R, Jayaraman S, Johns N, Jonas JB, Karthikeyan G, Kassebaum N, Kawakami N, Keren A, Khoo JP, King CH, Knowlton LM, Kobusingye O, Koranteng A, Krishnamurthi R, Laloo R, Laslett LL, Lathlean T, Leasher JL, Lee YY, Leigh J, Lim SS, Limb E, Lin JK, Lipnick M, Lipshultz SE, Liu W, Loane M, Ohno SL, Lyons R, Ma J, Mabweijano J, MacIntyre MF, Malekzadeh R, Mallinger L, Manivannan S, Marcenes W, March L, Margolis DJ, Marks GB, Marks R, Matsumori A, Matzopoulos R, Mayosi BM, McAnulty JH, McDermott MM, McGill N, McGrath J, Medina-Mora ME, Meltzer M, Mensah GA, Merriman TR, Meyer AC, Miglioli V, Miller M, Miller TR, Mitchell PB, Mocumbi AO, Moffitt TE, Mokdad AA, Monasta L, Montico M, Moradi-Lakeh M, Moran A, Morawska L, Mori R, Murdoch ME, Mwaniki MK, Naidoo K, Nair MN, Naldi L, Narayan KM, Nelson PK, Nelson RG, Nevitt MC, Newton CR, Nolte S, Norman P, Norman R, O'Donnell M, O'Hanlon S, Olives C, Omer SB, Ortblad K, Osborne R, Ozgediz D, Page A, Pahari B, Pandian JD, Rivero AP, Patten SB, Pearce N, Padilla RP, Perez-Ruiz F, Perico N, Pesudovs K, Phillips D, Phillips MR, Pierce K, Pion S, Polanczyk GV, Polinder S, Pope CA 3rd, Popova S, Porrini E, Pourmalek F, Prince M, Pullan RL, Ramaiah KD, Ranganathan D, Ravavi H, Regan M, Rehm JT, Rein DB, Remuzzi G, Richardson K, Rivara FP, Roberts T, Robinson C, De Leòn FR, Ronfani L, Room R, Rosenfeld LC, Rushton L, Sacco RL, Saha S, Sampson U, Sanchez-Riera L, Sanman E, Schwebel DC, Scott JG, Segui-Gomez M, Shahrzad S, Shepard DS, Shin H, Shivakoti R, Singh D, Singh GM, Singh JA, Singleton J, Sleet DA, Sliwa K, Smith E, Smith JL, Stapelberg NJ, Steer A, Steiner T, Stolk WA, Stovner LJ, Sudfeld C, Syed S, Tamburlini G, Tavakkoli M, Taylor HR, Taylor JA, Taylor WJ, Thomas B, Thomson WM, Thurston GD, Tleyjeh IM, Tonelli M, Towbin JA, Truelsen T, Tsilimbaris MK, Ubeda C, Undurraga EA, van der Werf MJ, van Os J, Vavilala MS, Venketasubramanian N, Wang M, Wang W, Watt K, Weatherall DJ, Weinstock MA, Weintraub R, Weisskopf MG, Weissman MM, White RA, Whitleford H, Wiersma ST, Wilkinson JD, Williams HC, Williams SR, Witt E, Wolfe F, Woolf AD, Wulf S, Yeh PH, Zaidi AK, Zheng ZJ, Zonies D, Lopez AD, Murray CJ, AlMazroa MA, Memish ZA. Years lived with disability (YLDs) for 1160 sequelae of 289 diseases and injuries 1990-2010: a systematic analysis for the Global Burden of Disease Study 2010. *Lancet* 2012; 380: 2163-96.
- [2] Gerstenfeld LC, Cullinane DM, Barnes GL, Graves DT, Einhorn TA. Fracture healing as a post-natal developmental process: molecular, spatial, and temporal aspects of its regulation. *J Cell Biochem* 2003; 88: 873-84.
- [3] Armocida F, Barfield WR, Hartsock LA. Conventional plate fixation of periarticular fractures. *J Surg Orthop Adv* 2009; 18: 163-9.
- [4] Lerner A, Stein H. Hybrid thin wire external fixation: an effective, minimally invasive, modular surgical tool for the stabilization of periarticular fractures. *Orthopedics* 2004; 27: 59-62.
- [5] Carr JB. Surgical techniques useful in the treatment of complex periarticular fractures of the lower extremity. *Orthop Clin North Am* 1994; 25: 613-624.
- [6] Mosekilde L, Ebbesen EN, Tornvig L, Thomsen JS. Trabecular bone structure and strength-remodelling and repair. *J Musculoskelet Neuro-nal Interact* 2000; 1: 25-30.
- [7] Carter DR, Hayes WC. Compact bone fatigue damage: a microscopic examination. *Clin Orthop Relat Res* 1977: 265-74.
- [8] Birkenhager-Frenkel DH, Nigg AL, Hens CJ, Birkenhager JC. Changes of interstitial bone thickness with age in men and women. *Bone* 1993; 14: 211-216.
- [9] Goff MG, Slyfield CR, Kummari SR, Tkachenko EV, Fischer SE, Yi YH, Jekir MG, Keaveny TM, Hernandez CJ. Three-dimensional characterization of resorption cavity size and location in human vertebral trabecular bone. *Bone* 2012; 51: 28-37.
- [10] Hernandez CJ. How can bone turnover modify bone strength independent of bone mass. *Bone* 2008; 42: 1014-1020.
- [11] McNamara LM, Van der Linden JC, Weinans H, Prendergast PJ. Stress-concentrating effect of resorption lacunae in trabecular bone. *J Biomech* 2006; 39: 734-741.

A mouse model to study cancellous fracture healing

- [12] Nunamaker DM. Experimental models of fracture repair. *Clin Orthop Relat Res* 1998; S56-65.
- [13] Chen WT, Han dC, Zhang PX, Han N, Kou YH, Yin XF, Jiang BG. A special healing pattern in stable metaphyseal fractures. *Acta Orthop* 2015; 86: 238-242.
- [14] Armocida F, Barfield WR, Hartsock LA. Conventional plate fixation of periarticular fractures. *J Surg Orthop Adv* 2009; 18: 163-169.
- [15] Lerner A, Stein H. Hybrid thin wire external fixation: an effective, minimally invasive, modular surgical tool for the stabilization of periarticular fractures. *Orthopedics* 2004; 27: 59-62.
- [16] Carr JB. Surgical techniques useful in the treatment of complex periarticular fractures of the lower extremity. *Orthop Clin North Am* 1994; 25: 613-624.
- [17] Mosekilde L, Ebbesen EN, Tornvig L, Thomsen JS. Trabecular bone structure and strength-remodelling and repair. *J Musculoskelet Neural Interact* 2000; 1: 25-30.
- [18] Agholme F, Li X, Isaksson H, Ke HZ, Aspenberg P. Sclerostin antibody treatment enhances metaphyseal bone healing in rats. *J Bone Miner Res* 2010; 25: 2412-2418.
- [19] McGee-Lawrence ME, Ryan ZC, Carpio LR, Karkar S, Westendorf JJ, Kumar R. Sclerostin deficient mice rapidly heal bone defects by activating beta-catenin and increasing intramembranous ossification. *Biochem Biophys Res Commun* 2013; 441: 886-890.
- [20] Han D, Han N, Xue F, Zhang P. A novel specialized staging system for cancellous fracture healing, distinct from traditional healing pattern of diaphysis cortical fracture. *Int J Clin Exp Med* 2015; 8: 1301-1304.
- [21] Teitelbaum SL. Bone resorption by osteoclasts. *Science* 2000; 289: 1504-1508.
- [22] Udagawa N, Takahashi N, Akatsu T, Tanaka H, Sasaki T, Nishihara T, Koga T, Martin TJ, Suda T. Origin of osteoclasts: mature monocytes and macrophages are capable of differentiating into osteoclasts under a suitable microenvironment prepared by bone marrow-derived stromal cells. *Proc Natl Acad Sci U S A* 1990; 87: 7260-7264.
- [23] Chang J, Wang Z, Tang E, Fan Z, McCauley L, Franceschi R, Guan K, Krebsbach PH, Wang CY. Inhibition of osteoblastic bone formation by nuclear factor-kappaB. *Nat Med* 2009; 15: 682-9.
- [24] Krum SA, Chang J, Miranda-Carboni G, Wang CY. Novel functions for NFkappaB: inhibition of bone formation. *Nat Rev Rheumatol* 2010; 6: 607-611.